Respiratory Research

RESEARCH Open Access

Activation of Nrf2 pathway by 4-Octyl itaconate enhances donor lung function in cold preservation settings

Xinliang Gao[1], Mingbo Tang[1], Jialin Li[1], Jianzun Ma[1], Zhengrui Liu[2] and Wei Liu[1*]

Abstract

Background Lung transplantation is the primary treatment for end-stage lung diseases. However, ischemia-reperfusion injury (IRI) significantly impacts transplant outcomes. 4-Octyl itaconate (4-OI) has shown potential in mitigating organ IRI, although its effects in lung transplantation require further exploration.

Methods BEAS-2B cells were used to model transplantation, assessing the effects of 4-OI through viability, apoptosis, and ROS assays. qRT-PCR analyzed cytokine transcription post-cold ischemia/reperfusion (CI/R). RNA sequencing and Gene Ontology analysis elucidated 4-OI's mechanisms of action, confirmed by Western blotting. ALI-airway and lung transplantation organoid models evaluated improvements in bronchial epithelial morphology and function due to 4-OI. ELISA measured IL-6 and IL-8 levels. Rat models of extended cold preservation and non-heart-beating transplantation assessed 4-OI's impact on lung function, injury, and inflammation.

Results Our findings indicate that 4-OI (100 μM) during cold preservation effectively maintained cell viability, decreased apoptosis, and reduced ROS production in BEAS-2B cells under CI/R conditions. It also downregulated pro-inflammatory cytokine transcription, including IL1B, IL6, and TNF. Inhibition of Nrf2 partially reversed these protective effects. In cold preservation solutions, 4-OI upregulated Nrf2 target genes such as NQO1, HMOX1, and SLC7A11. In ALI airway models, 4-OI enhanced bronchial epithelial barrier integrity and ciliary beat function after CI/R. In rat models, 4-OI administration improved lung function and reduced pulmonary edema, tissue injury, apoptosis, and systemic inflammation following extended cold preservation or non-heart-beating lung transplantation.

Conclusions Incorporating 4-OI into cold preservation solutions appears promising for alleviating CI/R-induced bronchial epithelial injury and enhancing lung transplant outcomes via Nrf2 pathway activation.

Keywords Lung transplantation, Ischemia-reperfusion injury, Primary graft dysfunction, Static cold storage, 4-octyl itaconate, E2-related factor 2

*Correspondence:
Wei Liu
l_w01@jlu.edu.cn
[1]Department of Thoracic Surgery, The First Hospital of Jilin University, Changchun 130021, China
[2]Changchun Yifu Jilin Province Academician Workstation, Changchun, China

© The Author(s) 2025. **Open Access** This article is licensed under a Creative Commons Attribution-NonCommercial-NoDerivatives 4.0 International License, which permits any non-commercial use, sharing, distribution and reproduction in any medium or format, as long as you give appropriate credit to the original author(s) and the source, provide a link to the Creative Commons licence, and indicate if you modified the licensed material. You do not have permission under this licence to share adapted material derived from this article or parts of it. The images or other third party material in this article are included in the article's Creative Commons licence, unless indicated otherwise in a credit line to the material. If material is not included in the article's Creative Commons licence and your intended use is not permitted by statutory regulation or exceeds the permitted use, you will need to obtain permission directly from the copyright holder. To view a copy of this licence, visit http://creativecommons.org/licenses/by-nc-nd/4.0/.

Background

Lung transplantation (LTx) remains the sole effective treatment for end-stage lung disease [1]. Despite advancements in donor lung harvest and preservation techniques, 10–25% of lung transplant recipients still experience primary graft dysfunction (PGD) post-surgery [2], leading to mortality within the first 30 days after the operation [3]. The risk of PGD has driven transplant clinicians to adopt stricter standards for donor lungs and shorter cold preservation time, consequently reducing donor lung utilization and creating logistical challenges in lung transplantation [4, 5]. Thus, research on alleviating PGD is a critical focus in lung transplantation.

The molecular mechanisms underlying PGD remain elusive. Nevertheless, it is recognized that cold ischemia followed by reperfusion (CI/R) instigates reactive oxygen species (ROS) production, leading to inflammation and cellular death. The prevailing standard for donor lung storage involves cold static preservation using a low-potassium dextran (LPD) solution at 4 °C [6]. This method decreases cellular energy metabolism, thereby extending the preservation and transport duration of donor lungs. However, it also predisposes the organs to oxidative stress and inflammation upon reperfusion [7–8]. Consequently, enhancing protection during cold preservation could improve post-transplant lung function. Itaconate, a metabolite of the tricarboxylic acid cycle, plays a pivotal role in regulating cellular immune responses and oxidative stress [9]. Additionally, 4-octyl itaconate (4-OI), a cell-permeable derivative of itaconate, mitigates inflammation and cell death by alkylating Keap1 to activate Nrf2 [10] or by modifying STING to downregulate IFN-β and TNF-α [11]. Furthermore, endogenous itaconic acid production, which is augmented by the enzyme IRG1 during cold preservation, has been demonstrated to enhance heart function post-heart transplantation [12]. Despite the unique anatomical features of the lungs—wherein the oxygen stored in the alveoli keeps cells relatively aerobic during lung harvest and preservation—they still face challenges such as ROS production and the release of inflammatory mediators. Consequently, ischemia-reperfusion injury (IRI) in lung transplantation differs from other organ transplants and non-transplant conditions, such as thromboembolism. This study explores whether exogenous 4-OI effectively preserves cold donor lungs, focusing on its protective effects and mechanisms in reducing oxidative stress and inflammation in vitro and in vivo during LTx CI/R injury.

Table 1 rt-QPCR primers used *for IL1B*, *IL6*, *IL8*, and *TNF* mRNAs

1) IL1B-F: ATGATGGCTTATTACAGTGGCAA
IL1B-R: GTCGGAGATTCGTAGCTGGA
2) IL6-F: ACTCACCTCTTCAGAACGAATTG
IL6-R: CCATCTTTGGAAGGTTCAGGTTG
3) IL8-F: ACTGAGAGTGATTGAGAGTGGAC
IL8-R: AACCCTCTGCACCCAGTTTTC
4) TNF-F: CCTCTCTCTAATCAGCCCTCTG
TNF-R: GAGGACCTGGGAGTAGATGAG
5) ACTB-F: ACTGGAACGGTGAAGGTGACA
ACTB-R: ATGGCAAGGGACTTCCTGTAAC

Methods

Cell culture model mimicking lung transplantation

Human bronchial epithelial (BEAS-2B) cells, acquired from Fuheng Biotechnology Co., Ltd. (Shanghai, China), were cultured in DMEM (ThermoFisher, USA) supplemented with 10% fetal bovine serum (FBS) (Gibco, USA) at 37 °C in a 5% CO^2 atmosphere. To mimic clinical LTx, the Toronto cell culture model was employed [13]. Upon reaching 80% confluency, the cell culture medium was replaced by 4 °C LPD solution with or without substance to be tested, and placed in a 4 °C airtight chamber with 50% oxygen for 24 h to simulate cold lung preservation. Subsequently, the cells were returned to their original culture conditions (DMEM + 10% FBS at 37 °C) for 4 h to simulate reperfusion. To study the protective effect of 4-OI and its mechanism, we added 4-OI (HY-112675, MCE ®) to LPD during cold storage.

Cell viability was assessed using a Cell Counting Kit (CCK)-8 (#MA0218-2) provided by Meilunbio Co. Limited (Dalian, China). Apoptosis and reactive oxygen species (ROS) production were evaluated using the Annexin V-FITC/PI apoptosis kit (#K2003) from APExBIO Technology LLC (Houston, USA) and the ROS assay kit (#CA1410) from Solarbio Science & Technology Co., Ltd. (Beijing, China). Quantitative real-time reverse transcription polymerase chain reaction (qRT-PCR) was used to quantify the mRNA levels of pro-inflammatory mediators, including IL-1B, IL-6, IL-8, and TNF, all produced by bronchial epithelial cells. The relative expression levels of target genes were calculated using the $2^{-\Delta\Delta Ct}$ method and normalized to ACTB. All primers used in this study are listed in Table 1. Transcriptome analysis was conducted on the Illumina NovaSeq platform by Shanghai Personalbio Technology Co., Ltd. Analysis of differentially expressed genes (DEGs) was performed using GENESCLOUD, a web tool of Personalbio (https://www.genescloud.cn/home). Western blotting was used to verify the DEGs found by transcriptome analysis.

Air-liquid culture model mimicking lung transplantation

The study was approved by the Institutional Ethics Committees of The First Hospital of Jilin University for tissue usage (approval number: 2024 – 479). Bronchial tissues were obtained from patients undergoing lobectomy for lung cancer. Lung cancer patients included in this study met the following criteria: (1) Postoperative pathology confirmed stage IA-IB NSCLC, with a tumor size of < 3 cm, and the lesion located in peripheral lung regions

distal to the subsegmental bronchi. (2) The patient had no history of smoking. (3) Preoperative lung CT scans showed no evidence of other pulmonary diseases, such as COPD, interstitial pneumonia, pneumonia, lung abscess, tuberculosis, or other infectious lung conditions. Segmental bronchial epithelial cells were isolated and cultured using established methods [14] and the STEMCELL Technologies (USA) protocol. During surgery, a normal segmental bronchus was excised from the lung lobe and stored in a transport preservation solution composed of DMEM/F-12 (Sigma, #D8437), 15 mM HEPES (Beyotime Biotechnology, Shanghai, China, #C0215), and Normocin (InvivoGen, USA, #ant-nr-05). This tissue was then transported to our laboratory.

In the laboratory, bronchial tissue was diced into pieces no larger than 2 mm in diameter on ice. The minced tissue was rinsed with D-PBS (Meilunbio, China, #MA0010) and digested at 37 °C for 60 min on an orbital shaker in 30 ml of a collagenase-containing preservation solution (Beyotime, China, #ST2303). After digestion, the tissue was strained through a 100 μm strainer and centrifuged at 1200 rpm for 5 min to collect primary bronchial epithelial cells. These cells were then cultured in PneumaCult™-Ex Plus Medium (STEMCELL Technologies, USA, #05040) seeded onto 0.4 μm Transwell inserts at passage two. They were maintained in submerged culture using PneumaCult™-Ex Plus Medium until reaching full confluency; the medium in the basal chamber was then switched to PneumaCult™-ALI medium (STEMCELL Technologies, #05001), while the medium in the apical chamber was removed. The cells were cultured at an air-liquid interface for 28 days, with media changes every other day and weekly D-PBS washes of the apical chamber to remove mucus, promoting complete differentiation.

To simulate the CI/R procedure during lung transplantation, the medium in the basal chamber was replaced with LPD, and the inserts were stored in an airtight chamber with 50% O^2 at 4℃ for 24 h. The LPD was then replaced with PneumaCult™-ALI medium, and the inserts were incubated at 37℃ with 5% CO^2 for 24 h. Bright-field microscopy was utilized to observe the growth of the bronchial epithelium, noting ciliary movement and mucus secretion.

Bronchial epithelial function assessment

The primary roles of the bronchial epithelium encompass ciliary movement, maintaining the integrity of the airway barrier, and the secretion of inflammatory mediators. To assess the function of the bronchial epithelial barrier, we employed several methods: microscopic measurement of ciliary beat frequency (CBF), transepithelial electrical resistance (TEER) and a FITC-dextran permeation assay to assess permeability and barrier integrity, and the quantification of secretion and expression of key pro-inflammatory mediators, namely IL-6 and IL-8. Each experimental group consisted of five samples.

CBF measurement

Before measurement, the cells were washed with D-PBS, adding 0.2 mL of D-PBS to the top chamber and 0.5 mL to the bottom chamber. The ciliary activity was then recorded for 30 s at room temperature using a high-speed camera (ORCA-Flash4.0 V3) at 40× magnification. Each sample was measured randomly across three visual fields, and the average CBF was calculated for each well.

Transepithelial electrical resistance (TEER) measurement

TEER was measured weekly after airlifting to assess bronchial epithelial barrier function, particularly during CI/R. Measurements were conducted using the EVOM 3 and STX-2 plus electrode (World Precision Instrument, USA). Before recording, the media on the apical and basal sides of the Transwell® insert was replaced with D-PBS, and the electrode was submerged in D-PBS to equilibrate. Cells were removed from the incubator and allowed to reach room temperature before measurements.

TEER values were calculated using the formula: TEER = (Raw value − blank value, i.e., without cells) * 0.33 cm^2, which is the growth surface area of the insert. Each well was measured three times, and the average was taken. The results are presented as the mean ± SD for each cell group.

Fluorescein isothiocyanate (FITC)-Dextran assay

The medium in the Transwell® chambers was aspirated, followed by adding 0.5 mL of medium to the top chamber and 1 mL to the bottom chamber. FITC-labeled dextran (1 mg/mL) with a molecular weight of 4 kDa (MedChemExpress, USA, #HY-128868 A) was introduced into the apical chamber. Thirty minutes later, D-PBS was collected separately from the top and bottom chambers. The fluorescence signal of the D-PBS was then quantified using a fluorescence microplate reader at an excitation wavelength of 485 nm and an emission wavelength of 538 nm.

Secretion of IL-6 and IL-8 by bronchial epithelium

The medium from the basal chamber was centrifuged at 500×g for 5 min. The levels of IL-6 and IL-8 in the medium were then determined using human ELISA kits (Beyotime Biotechnology, #PI325 and #PI641).

Rat orthotopic lung transplantation model

All animal procedures were approved and performed according to the protocols established by the Institutional Animal Care and Use Committee of The First Hospital of Jilin University (approval number: 2023[0636]).

Rat orthotopic left lung transplantation was performed to create lung transplantation models with extended cold preservation or under non-heart-beating conditions, as previously described [15, 16]. In brief, donor rats were anesthetized with isoflurane, trachea intubated with a 14 G catheter, and ventilated with a tidal volume of 10 mL/kg, PEEP of 2 cm H_2O, FiO_2 of 0.5, and 80 breaths per minute in the supine position. Following a laparotomy, 1000 USP units/kg of heparin and 30 mg/kg of methylprednisolone were injected into the inferior vena cava (IVC). After 3 min, a median sternotomy was then performed to open the thoracic cavity.

To establish the extended cold preservation model, the lungs were flushed with 20 mL of LPD solution containing either 4-OI or dimethylsulfoxide (DMSO), a vehicle control through the main pulmonary artery using gravity flow (15 cm H_2O). In the non-heart-beating model, the rats were euthanized by cutting the IVC. One hour later, the lungs were flushed using the same method as in the extended cold preservation model. The heart and lung blocks were harvested, and three cuffs (bronchial, pulmonary vein, and pulmonary artery) were placed on the grafts for anastomoses. The donor lung was stored on ice in LPD with 4-OI or DMSO at 4℃ for 12 h (as an extended cold preservation model) or 3 h (as a non-heart-beating model) until anastomosis.

Meanwhile, as previously described, recipient rats were anesthetized and intraperitoneally injected with triple immunosuppressive agents. Ventilation was established at FiO_2 of 1.0, and the recipient rats were placed in the lateral position. A left thoracotomy was performed to expose the left hilum, and the vessel structures were clamped. The left lung was removed, and the lung graft was anastomosed using a cuff technique. The transplanted lung was then reperfused. The rats' chest cavities were closed, and they were allowed to recover. Two hours and forty-five minutes after transplantation, the recipient rats were re-anesthetized and underwent a median sternotomy. Three hours post-reperfusion, blood samples were collected for blood gas analysis. These samples were taken from the left pulmonary veins of the transplanted lung to measure the partial pressure of oxygen to fraction of inspired oxygen ratio (PO_2/FiO_2 (P/F)) and from the right auricle for cytokine analysis.

Subsequently, the animals were euthanized. The transplanted lung was bisected for detailed analysis: the upper sections were designated for histological examinations, and the lower sections were analyzed to assess the wet-to-dry weight ratio (W/D).

Measurement of wet-to-dry-weight (W/D) ratio

The W/D ratio of the lung tissue was measured to assess pulmonary edema [17]. Wet weight was determined within 5 min of procurement. The lung tissue was then dried in an oven at 80 °C for 72 h, and the dry weight was measured. W/D ratio equals wet weight/ dry weight.

Histological analysis and lung injury score

The lower section of the transplanted left lung was fixed in 10% buffered formalin, embedded in paraffin, sectioned into 5-μm-thick slices, and stained using standard hematoxylin and eosin (H&E) staining. A pathologist, blinded to the study groups, performed a semiquantitative assessment of lung injury based on previously described criteria [18]. The scoring criteria included alveolar hemorrhage (the presence of red blood cells in air spaces), vascular congestion (more than 75% of alveolar septa occupied with red blood cells), alveolar fibrin (the presence of fibrin in alveoli), and neutrophil infiltration (presence of neutrophils in the lung tissue). Each criterion was graded on a 4-level scale of abnormalities: normal appearance (0%) as 0, mild (< 10%) as 1, moderate (10–50%) as 2, and severe (> 50%) as 3.

Immunofluorescence staining for assessing lung cell death

As previously described, apoptotic cells in the lung tissue were identified and quantified through immunostaining using the terminal deoxynucleotidyl transferase dUTP nick end labeling (TUNEL) method [19]. The TUNEL reagent (APExBIO, #K1133) was diluted at 1:100 and applied to the tissue sections for 20 min at room temperature. Nuclei were stained using 4′,6-diamidino-2-phenylindole at a concentration of 2 μg/mL. Immunofluorescence was assessed with a fluorescence microscope, and images were captured from 10 randomly selected high-power fields per section.

Measurement of cytokine expressions in plasma samples

Before the rats were sacrificed, 1 mL of blood was collected from each rat. Allowing the blood samples to sit for 20 min, they were centrifuged at 2000×g for 10 min to separate the serum. The collected serum samples were then analyzed for determining cytokine levels using ELISA kits specific for IL-1β, IL-6, IL-8, and TNFα provided by Biyuntian (China, #PI303, #PI328, and #PT516), as well as Soleibao Life Science, (Beijing, China, #SEKR-0071).

Statistical analysis

All statistical analyses were conducted using GraphPad Prism version 10.1.2. The data were checked for normality using the Shapiro–Wilk test and analyzed parametrically. Statistical comparisons were made using a one-way analysis of variance, followed by Fisher's LSD post hoc test. A P value of less than 0.05 was considered to indicate statistical significance.

Results

Enhancing cellular resilience: 4-OI's protective role in CI/R injury

We investigated whether 4-OI could mitigate cold CI/R-induced impairment in lung epithelial cells. Using a CI/R cell culture model with BEAS-2B cells, we administered escalating concentrations of 4-OI (ranging from 0 to 400 μM) during the preservation (CI) or post-rewarming (R) phases. Cell viability was assessed using the CCK-8 assay after 4 h of rewarming. As illustrated in Fig. 1A, there was a significant decline in BEAS-2B cell viability following CI/R. Adding 4-OI during CI provided a dose-dependent protective effect on BEAS-2B cell viability after CI/R, with 100 μM as the optimal concentration for inclusion in the cold preservation solution. While adding 50 μM and 100 μM 4-OI post-rewarming (R) improved BEAS-2B cell viability post-CI/R, its effectiveness was less pronounced than its use during CI. Cell viability decreased beyond 100 μM, as shown in Fig. 1B. Therefore, 100 μM of 4-OI was chosen for subsequent experiments in a cold LPD solution.

To preliminarily determine if 4-OI in the cold preservation solution could enhance BEAS-2B cell viability post-CI/R through Nrf2 pathway activation, we also introduced 2 μM of ML385, a potent Nrf2 inhibitor, into the cold preservation solution. Results showed that ML385 alone had no significant effect on BEAS-2B cell viability post-CI/R but partially antagonized the protective effect of 4-OI on cell viability (Fig. 1C). Brightfield microscopy confirmed a substantial loss of BEAS-2B cells post CI/R, with 4-OI reducing this decline, though this was partially reversed by ML385 (Fig. 1D).

Unlocking cellular protection: 4-OI's Nrf2 activation guards BEAS-2B Post CI/R

To delve deeper into 4-OI's shielding mechanism against CI/R harm during cold preservation, we conducted intracellular transcriptome (RNA-sequencing) analysis on BEAS-2B cells rewarmed after 24 h in either LPD or

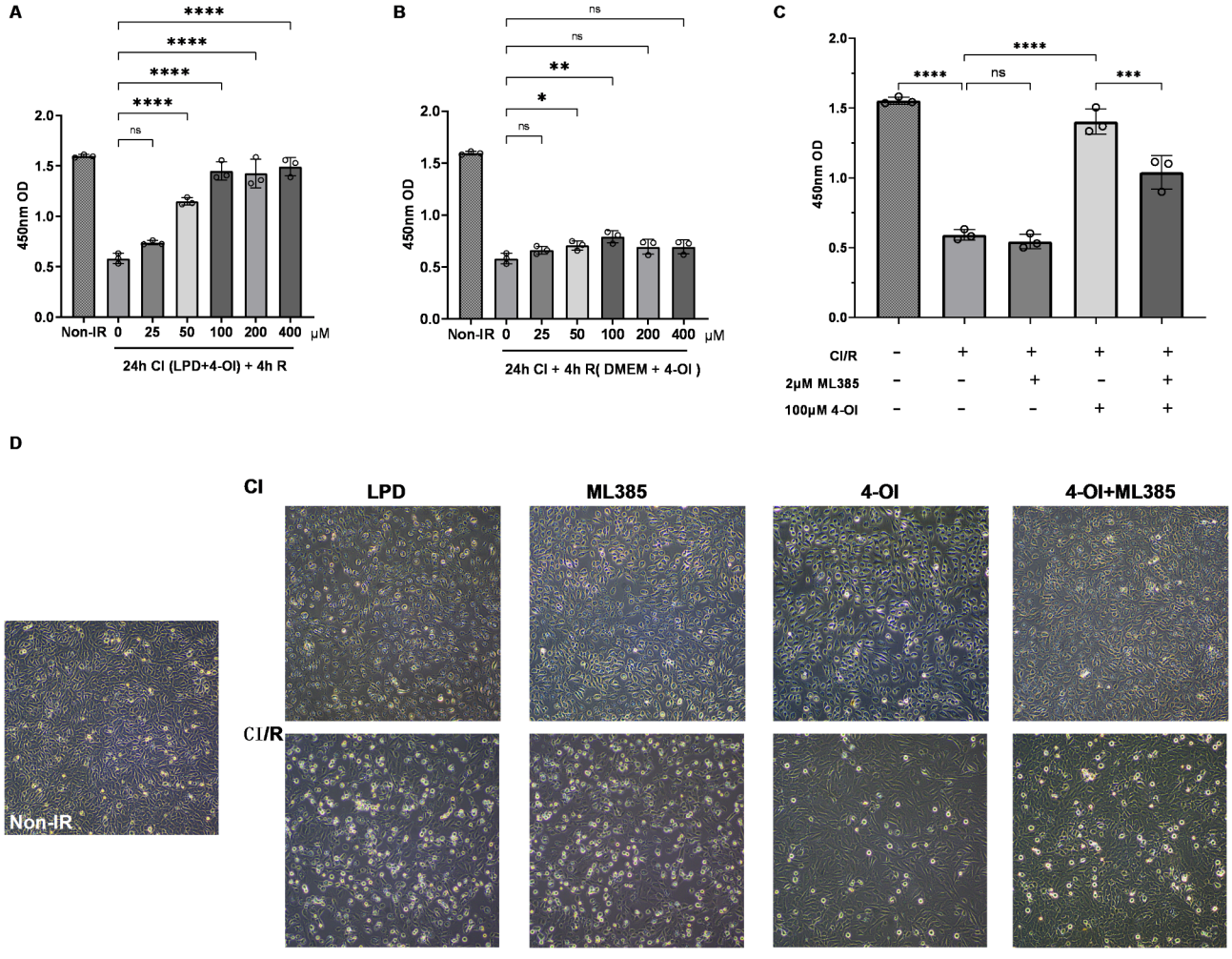

Fig. 1 Impact of 4-OI in preservation solution on BEAS-2B cell viability Post CI/R

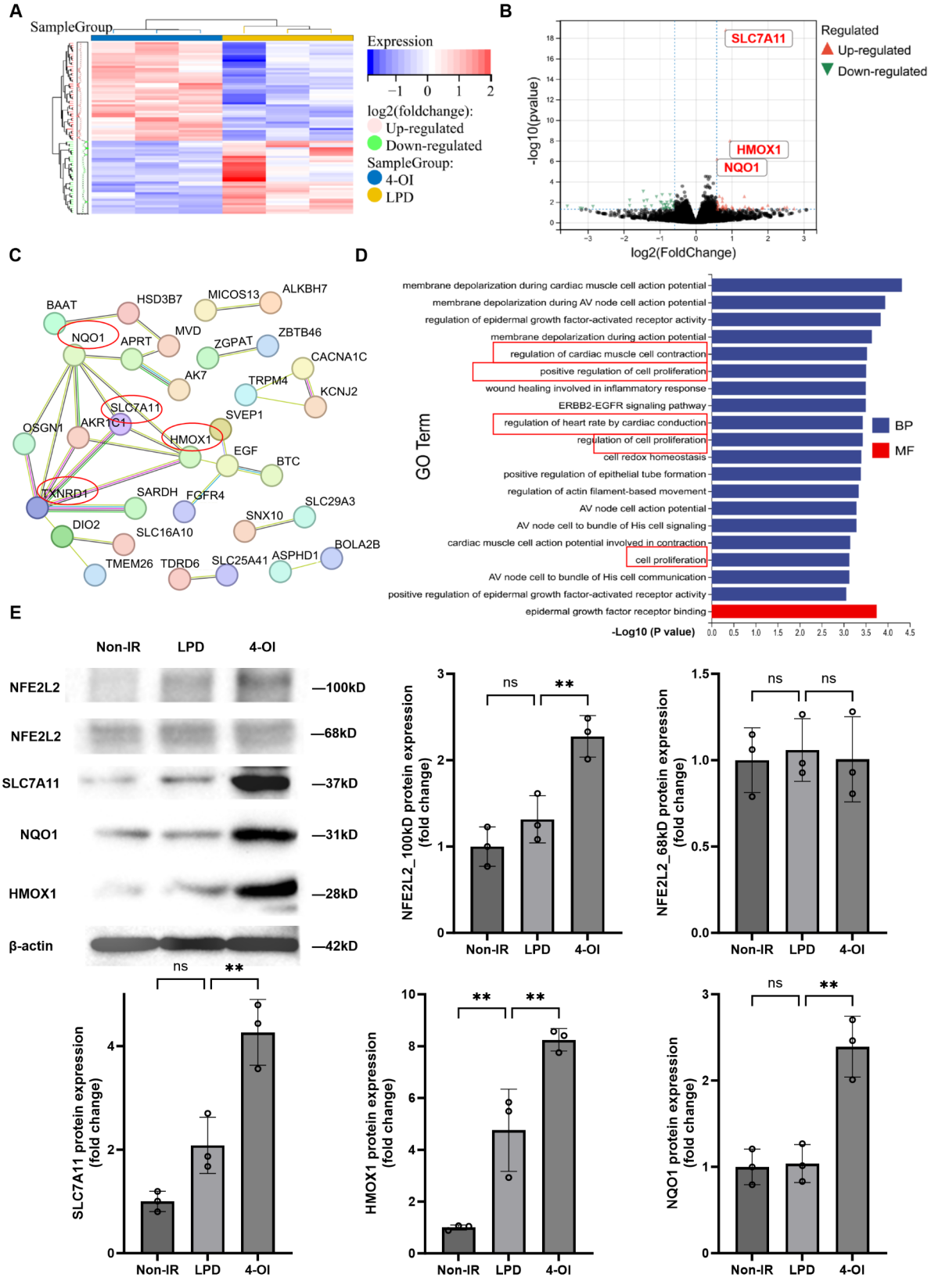

Fig. 2 (See legend on next page.)

(See figure on previous page.)

Fig. 2 Impact of 4-OI in Cold Preservation Solution on Transcriptome of BEAS-2B Cells Post CI/R. **A**. Heatmap plot of DEGs between 4-OI and LPD alone cold preservation for BEAS-2B post CI/R. **B**. Volcano plot of DEGs, with Nrf2 downstream genes highlighted.**C**. Protein-Protein Interaction (PPI) network of DEGs, emphasizing genes associated with redox homeostasis. **D.** Gene Ontology (GO) enrichment analysis of DEGs, indicating pathways pertaining to redox regulation, inflammatory response, and proliferation. E. Relative protein expression levels of Nrf2, SLC7A11, NQO1, and HMOX1 in BEAS-2B cells post CI/R. Data presented as mean ± standard deviation. Normal distribution of data verified. Statistical analysis was conducted via one-way ANOVA, with significance denoted as $^{*}P < 0.05$, $^{**}P < 0.01$, $^{***}P < 0.001$, $^{****}P < 0.0001$

LPD supplemented with 100 μM 4-OI. Differential gene expression analysis unveiled that cold preservation with LPD + 100 μM 4-OI could upregulate 46 genes and downregulate 34 genes in BEAS-2B cells post CI/R compared to LPD alone (Fig. 2A). Notably, downstream genes of Nrf2, including *SLC7A11*, *HMOX1*, and *NQO1*, exhibited significant upregulation (Fig. 2B). Protein-protein interaction (PPI) analysis revealed interactions among differentially expressed genes (DEGs), prominently featuring a network of 19 DEGs primarily associated with redox homeostasis maintenance, such as *TXNRD1*, *SLC7A11*, *HMOX1*, and *NQO1* (Fig. 2C).

Gene Ontology (GO) enrichment analysis highlighted enrichment in pathways related to regulation of redox homeostasis, inflammatory response, and proliferation regulation (Fig. 2D). Western blot (WB) results demonstrated that CI/R elevated HMOX1 expression only compared to BEAS-2B cells without CI/R, whereas the addition of 4-OI to the cold preservation solution notably enhanced Nrf2 expression and its key downstream genes: SLC7A11, HMOX1, and NQO1 compared to the group in the absence of 4-OI (Fig. 2E). In essence, our findings suggest that 4-OI potentially induces the expression of downstream antioxidant stress proteins via Nrf2 activation, thereby mitigating oxidative stress, apoptosis, and inflammatory responses to alleviate cellular ischemia-reperfusion injury.

Mitigating oxidative stress, apoptosis, and inflammation: 4-OI's protective role in CI/R-Induced damage to BEAS-2B through activating Nrf2

In cellular contexts, ROS stands as a cardinal indicator of oxidative stress. To furnish further evidence supporting the potential of 4-OI in the preservation solution to mitigate oxidative stress inflicted by CI/R and subsequently curtail cellular apoptosis and inflammatory responses, we scrutinized ROS production, apoptosis rates, and the expression of inflammatory mediators in BEAS-2B cells post-CI/R.

Initially, the CI/R process manifested an augmentation in the transcription of key pro-inflammatory mediators' mRNA in BEAS-2B cells, such as *IL1B*, *IL6*, *IL8*, and *TNF*. 4-OI in the preservation solution significantly reduced the mRNA expression levels of *IL1B*, *IL6*, and *TNF* in BEAS-2B cells following CI/R. However, the suppression of *IL1B* and *TNF* by 4-OI was partially reversed by adding ML385. In contrast, *IL8* transcription remained unaffected by CI/R (Fig. 3A).

Moreover, CI/R induced an increase in ROS production within BEAS-2B cells. Incorporating 4-OI into the cold preservation solution effectively decreased ROS production, although this effect was somewhat mitigated by ML385 (Fig. 3B).

Lastly, CI/R led to an increase in apoptosis among BEAS-2B cells. The inclusion of 4-OI in the preservation solution resulted in a reduction in apoptotic cell numbers. However, the anti-apoptotic effect of 4-OI was countered by the addition of ML385 (Fig. 3C).

Preserving bronchial epithelial Integrity: 4-OI's role in mitigating CI/R-Induced morphological disruption

To reveal the effects of CI/R and 4-OI on bronchial epithelial morphology and function, we applied the air-liquid culture model to simulate the changes in bronchial epithelium during lung transplantation. Under bright-field microscopy, the aftermath of CI/R unveiled a loss of bronchial epithelial uniformity within the inserts, with discernible alterations in morphology signifying ciliary epithelium impairment. Remarkably, 4-OI administration significantly restored airway epithelium uniformity post CI/R and mitigated morphological disruptions (Fig. 4A).

H&E staining further elucidated the repercussions of CI/R, characterized by a reduction in airway epithelial cilia density, shortened cilia length, and increased mucus secretion. However, incorporating 4-OI during cold preservation effectively shielded against CI/R-induced alterations in epithelial cilia length and density (Figs. 4B and 5A). These findings underscore the protective prowess of 4-OI in safeguarding bronchial epithelial morphology against CI/R-induced disruption.

Enhancing bronchial epithelial function Post CI/R: 4-OI's cold preservation solution intervention

Following CI/R, although bronchial epithelial thickness has not changed, a reduction in bronchial epithelial cilia length and CBF is observed using ALI model (Fig. 5A, B and C). Notably, including 4-OI in the cold preservation solution effectively mitigates CI/R-induced disruptions in CBF (Fig. 5C). Concurrently, CI/R damages the bronchial epithelial barrier, which is evident through decreased TEER and heightened permeability to dextran. Adding 100 μM 4-OI to LPD for cold preservation attenuates CI/R-induced disruptions in bronchial epithelial

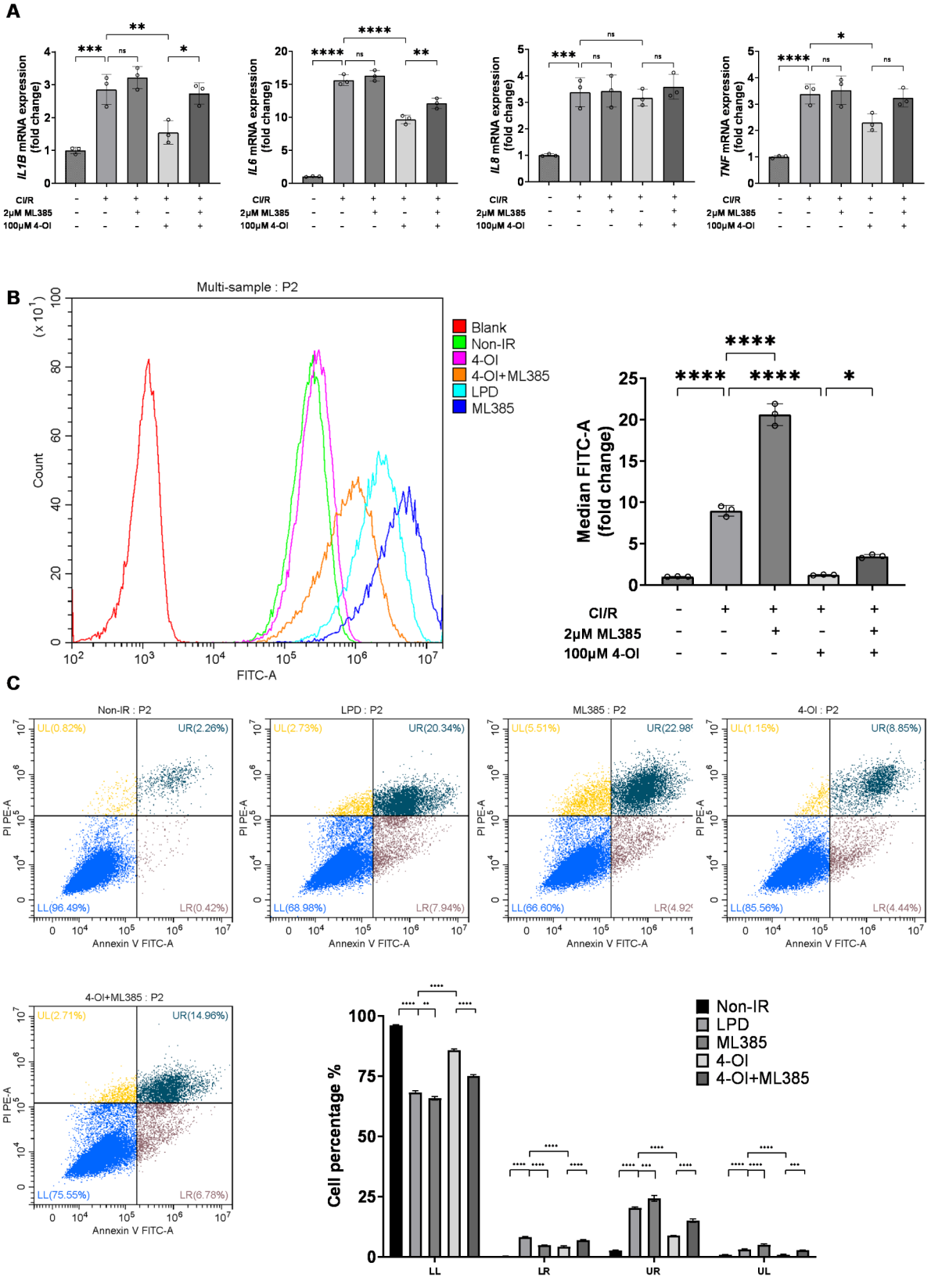

Fig. 3 (See legend on next page.)

(See figure on previous page.)

Fig. 3 Impact of 4-OI and ML385 in Cold Preservation Solution on Pro-inflammatory Mediators, ROS Production, and Apoptosis in BEAS-2B Cells Post CI/R. A. Influence of 4-OI and ML385 in preservation solution on transcription levels of *IL1B*, *IL6*, *IL8*, and *TNF* mRNA.**B**. Influence of 4-OI and ML385 in cold preservation solution on ROS production in BEAS-2B cells post CI/R **C**. Impact of 4-OI and ML385 in preservation solution on apoptosis in BEAS-2B cells post CI/R.Data presented as mean ± standard deviation. Normal distribution of data verified. Statistical analysis was conducted via one-way ANOVA, with significance denoted as $^{*}P < 0.05$, $^{**}P < 0.01$, $^{***}P < 0.001$, $^{****}P < 0.0001$

barrier function (Fig. 5D and E). Moreover, CI/R triggers an upsurge in the secretion of pro-inflammatory mediators by the bronchial epithelium, including IL-6 and IL-8. However, while 4-OI in the preservation solution ameliorates the increase in IL-6 secretion, its effect on IL-8 is less pronounced. The comprehensive impact of 4-OI in the preservation solution on airway epithelial morphology and function is delineated in Table 2.

Preservation solution fortification: 4-OI shields transplanted lung morphology and function during extended cold preservation

In order to observe the protection of 4-OI on the function and morphology of transplanted lungs, we used left lung transplantation in rats to establish EC and NHB models. Upon comparing the functionality of transplanted lungs following 12 h of preservation with LPD + 4-OI against LPD alone, notable differences emerged. Gross examination revealed diminished damage in transplanted lungs subjected to extended cold preservation with LPD + 4-OI in contrast to LPD alone (Fig. 6).

Histological analysis via H&E staining unveiled lighter alveolar hemorrhage, reduced vascular congestion, diminished alveolar fibrin, and neutrophil infiltration in transplanted lungs preserved with LPD + 4-OI, in comparison to the LPD preservation group (Figs. 6 and 8C). TUNEL staining further corroborated these findings, showcasing decreased apoptotic cell numbers in lungs post-transplantation with 4-OI in the preservation solution (Figs. 6 and 8D).

Furthermore, the addition of 4-OI to the preservation solution effectively improved the P/F ratio (Fig. 8A), reduced the W/D ratio (Fig. 7B), and mitigated serum IL-1β and TNFα levels in transplanted lungs following extended cold preservation (Fig. 8E and H).

Preservation of transplanted lung morphology and function after non-heart beating with 4-OI

We performed a comparative study using LPD with and without the addition of 4-OI, employing models that included 1-hour cardiac arrest, 3-hour cold preservation, and 3-hour reperfusion. Consistent with findings in the EC model, the inclusion of 4-OI in the LPD preservation solution mitigated morphological damage in NHB model transplanted lungs, as indicated by lower lung injury scores and a reduced number of apoptotic cells (refer to Figs. 7 and 8C and D). Additionally, 4-OI improved oxygenation function (Fig. 8A) and reduced pulmonary edema (Fig. 8B), typically induced by ischemia-reperfusion injury in the transplanted lungs. Moreover, supplementation with 4-OI was associated with decreased serum levels of IL-1β (illustrated in Fig. 8E) and IL-6 (displayed in Fig. 8F). Detailed morphological and functional parameters for both EC and NHB transplanted lungs are summarized in Table 3.

Discussion

In this study, we investigated the role of 4-OI in mitigating IRI in lung transplantation. Our findings demonstrated that 4-OI effectively alleviates oxidative stress, inflammation, and apoptosis associated with cold ischemia and reperfusion (CI/R) injury. Mechanistically, 4-OI exerts its protective effects by activating the Nrf2 signaling pathway, leading to the upregulation of antioxidant and cytoprotective genes such as HMOX1, NQO1, and SLC7A11. These findings align with previous research demonstrating the role of 4-OI in addressing various injuries such as infection [20, 21], inflammation [22–26], autoimmunity [27, 28], physicochemical damage [29–31], oxidative stress injury [32], and IRI [33], including its effects in acute kidney injury [34], osteoarthritis [35], and cardiovascular damage [36, 37] through similar Nrf2-mediated pathways. Given that lung transplantation involves unique characteristics of ischemia-reperfusion injury, particularly cold IRI with incomplete hypoxia, it is essential to validate the protective effects of 4-OI specifically within this context. This study is the first to extend these findings to lung transplantation, highlighting a novel application of 4-OI through its incorporation into cold preservation solutions. By focusing on lung transplantation-specific challenges, our research emphasizes the potential of 4-OI to address the distinct pathophysiology of cold IRI in lung grafts.

Previous studies have shown that 4-OI modulates the inflammatory response by alkylating Keap1, thereby releasing and activating Nrf2. Once activated, Nrf2 translocates to the nucleus and initiates the transcription of genes involved in oxidative stress regulation and cellular protection including NQO1 [38], HO-1 [36, 37], SLC7A11 [39, 40]. In our study, transcriptomic analysis revealed that 4-OI treatment during cold preservation significantly upregulated Nrf2-dependent genes. This was further validated through Western blot analysis, which showed increased protein levels of Nrf2 and its downstream targets in bronchial epithelial cells exposed to CI/R. Consistent with these findings, inhibition of Nrf2

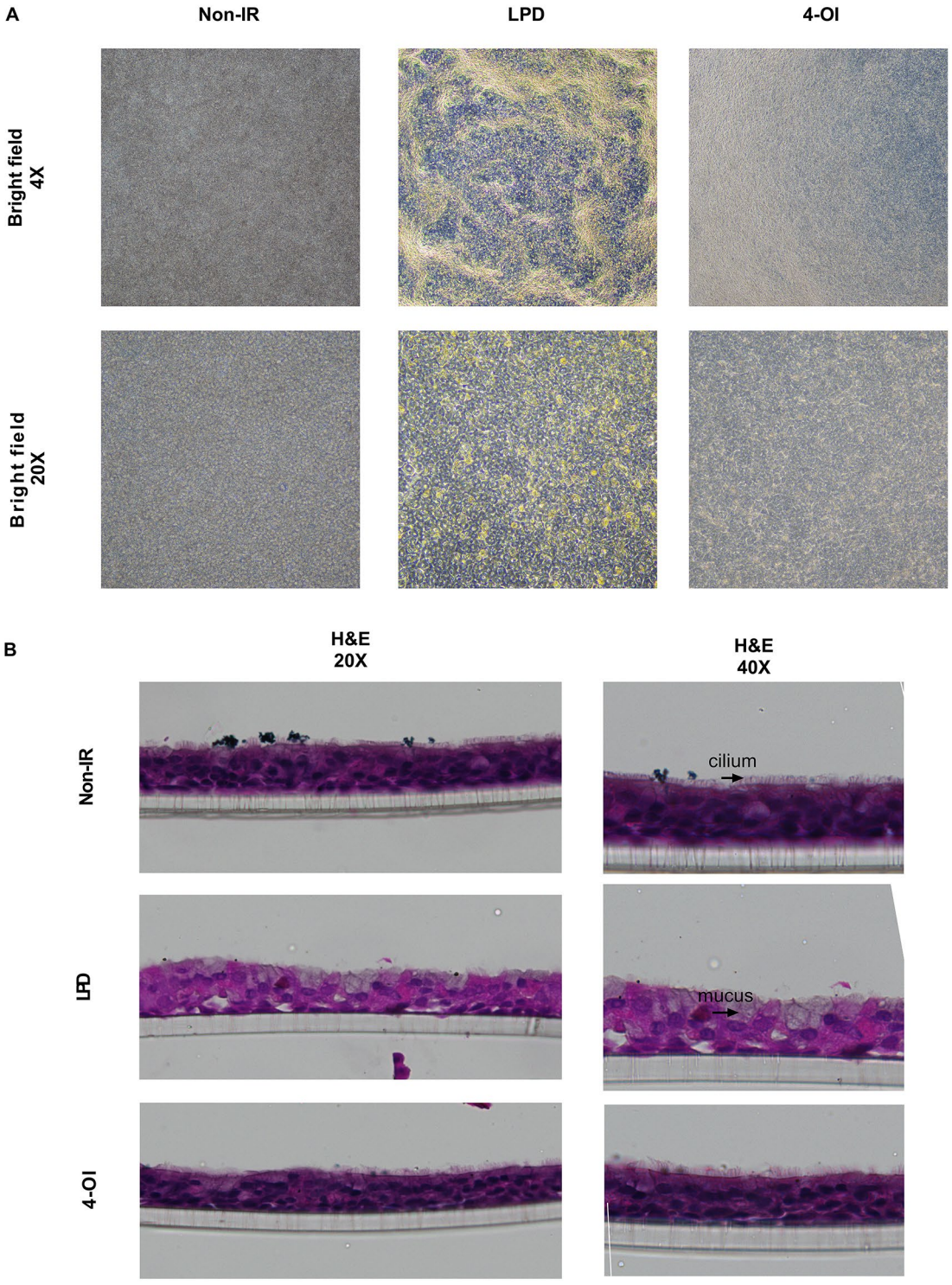

Fig. 4 Impact of 4-OI in preservation solution on aLI-airway morphology

with ML385 partially reversed the protective effects of 4-OI, confirming that the Nrf2 pathway is a critical mediator of 4-OI's benefits. These results reinforce the role of 4-OI as a potent activator of Nrf2 and support its potential use as an intervention to mitigate IRI in organ transplantation settings.

This study's innovation lies in its application of 4-OI through cold preservation solutions to improve lung

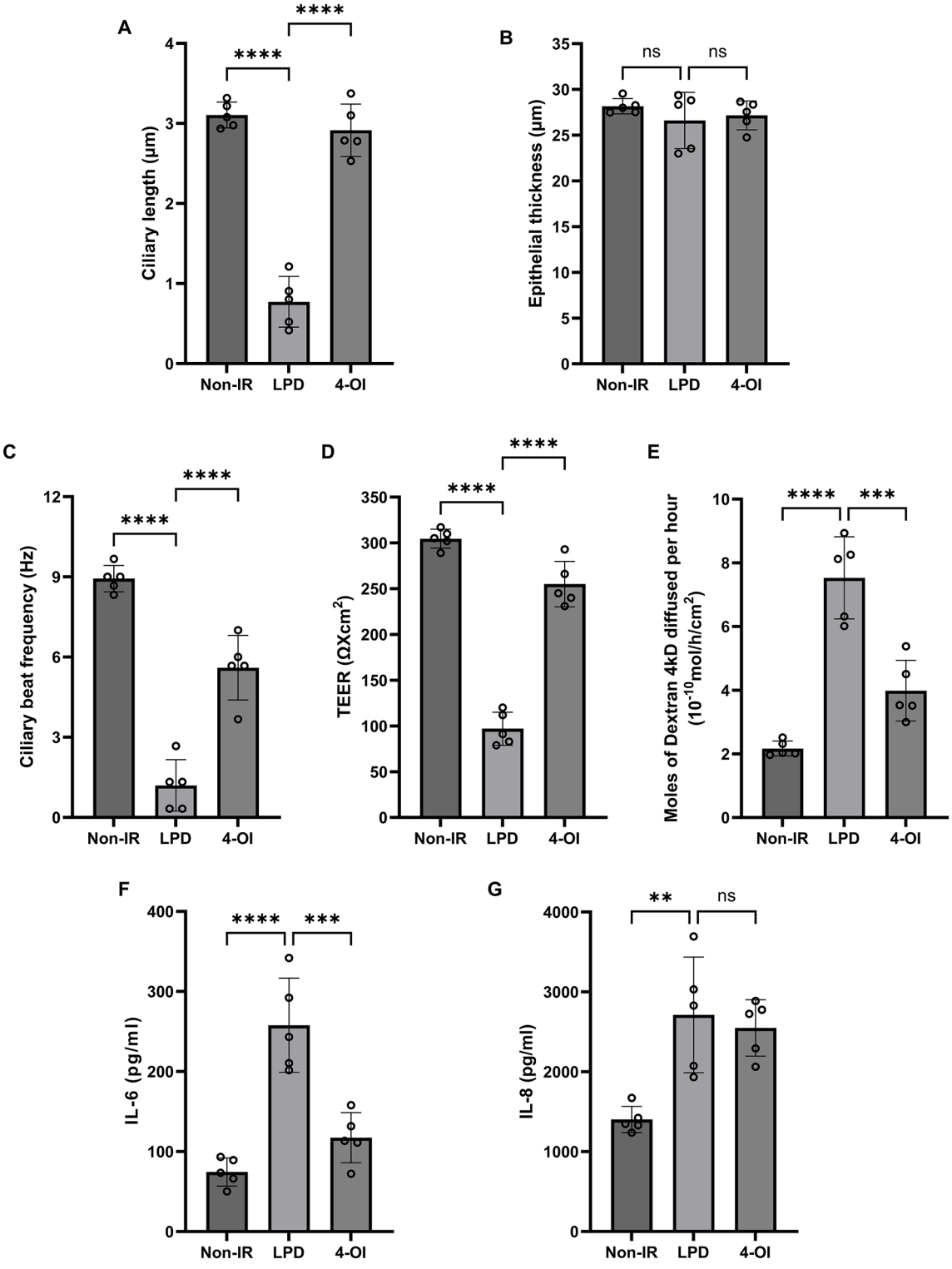

Fig. 5 Impact of 4-OI in Cold Preservation Solution on Bronchial Epithelial Morphology and Function. **A**. measurement of cilia length, **B**. assessment of epithelial thickness, **C**. analysis of cilia oscillation frequency, **D**. evaluation of TEER, **E**. assessment of permeation of 4 kD Dextran, **F**. quantification of IL-6 secretion, and **G**. quantification of IL-8 secretion. Data presented as mean ± standard deviation. Normal distribution of data verified. Statistical analysis was conducted via one-way ANOVA, with significance denoted as $^{*}P < 0.05$, $^{**}P < 0.01$, $^{***}P < 0.001$, $^{****}P < 0.0001$

Table 2 Enhancing airway epithelial morphology and function with preservation solution containing 4-OI

Bronchial epithelium	Non-IR	LPD	4-OI	LPD vs. Non-IR	4-OI vs. LPD
Ciliary length (μm)	3.11 ± 0.16	0.77 ± 0.32	2.91 ± 0.33	< 0.0001	< 0.0001
Epithelial thickness (μm)	28.16 ± 0.85	26.61 ± 3.08	27.17 ± 1.57	0.4464	0.8956
CBF (Hz)	8.93 ± 0.50	1.20 ± 0.96	5.60 ± 1.21	< 0.0001	< 0.0001
TEER (Ω*cm^2)	304.60 ± 10.41	97.00 ± 18.10	255.00 ± 24.83	< 0.0001	< 0.0001
Dextran diffusion (10–10 mol/h/cm^2)	2.17 ± 0.24	7.53 ± 1.29	3.98 ± 0.95	< 0.0001	0.0001
IL-6 (pg/ml)	74.45 ± 17.54	257.82 ± 58.87	117.26 ± 31.36	< 0.0001	0.0002
IL-8 (pg/ml)	1402.42 ± 164.89	2711.97 ± 723.84	2549.03 ± 352.90	0.0002	0.9632

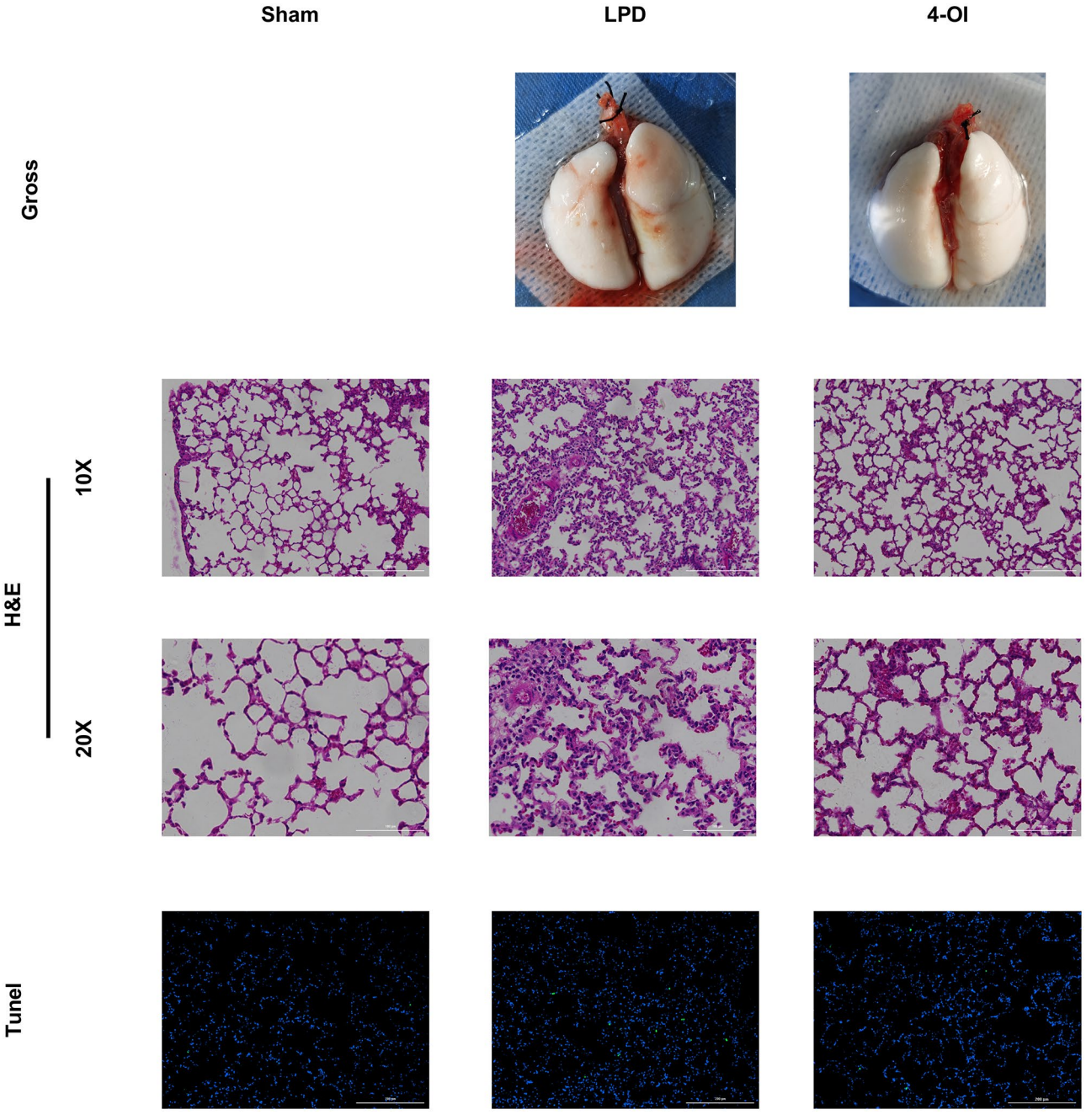

Fig. 6 Protective Effect of 4-OI in preservation solution on EC transplanted lung

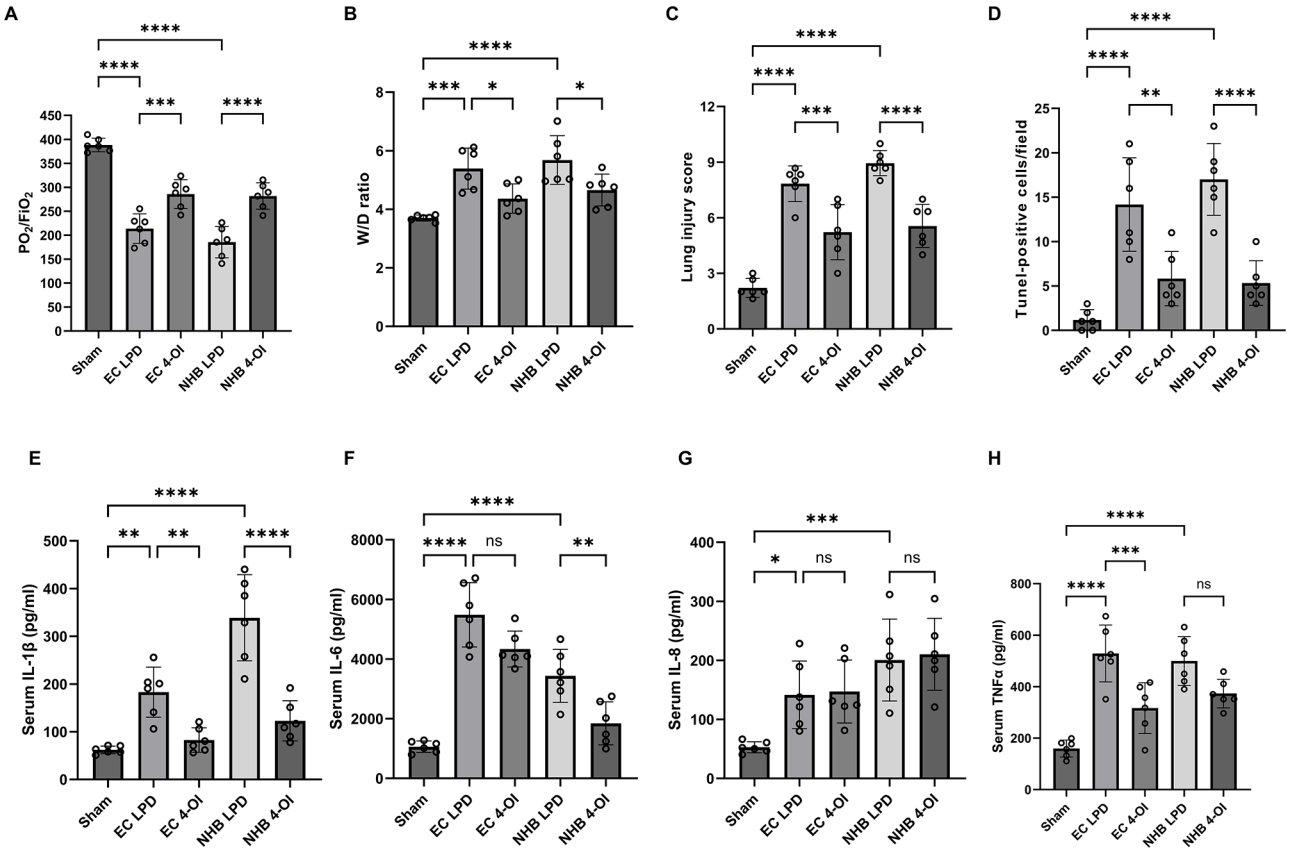

Fig. 8 Impact of 4-OI in Cold Preservation Solution on Protection against Transplant Lung Injury and Release of Pro-inflammatory Mediators. **A**. Ratio of partial pressure of oxygen (PO2) to fraction of inspired oxygen (FiO2)(P/F), **B**. Lung wet-to-dry weight ratio (W/D), **C**. Lung injury score, **D**. Number of Tunel-positive cells, **E**. Serum Interleukin-1β (IL-1β) level, **F**. Serum Interleukin-6 (IL-6) level, **G**. Serum Interleukin-8 (IL-8) level, and **H**. Serum Tumor Necrosis Factor (TNF) level. Data presented as mean ± standard deviation. Normal distribution of data verified. Statistical analysis was conducted via one-way ANOVA, with significance denoted as $^{*}P < 0.05$, $^{**}P < 0.01$, $^{***}P < 0.001$, $^{****}P < 0.0001$

transplant outcomes. Unlike previous approaches that relied on systemic administration, the localized inclusion of 4-OI in low-potassium dextran (LPD) solutions provides a targeted and practical method for enhancing donor lung protection during storage and transport. By adding 4-OI to the preservation solution, we observed improved bronchial epithelial barrier function, reduced oxidative damage, and decreased pro-inflammatory cytokine production in both in vitro and in vivo models. Furthermore, rat models of lung transplantation demonstrated improved oxygenation (P/F ratio), reduced pulmonary edema (W/D ratio), and lower lung injury scores in grafts preserved with 4-OI-enriched solutions compared to standard LPD solutions. These findings underscore the feasibility of incorporating 4-OI into clinical-grade preservation solutions as a strategy to enhance donor lung viability and transplant success.

The application of the air-liquid interface (ALI) model in this study represents an innovative approach to lung transplantation research. Traditional models for investigating lung transplantation include 2D cell culture systems and animal models. While 2D cell culture models offer simplicity, cost-effectiveness, and high-throughput capabilities, they lack the structural complexity and functional characteristics of airway epithelium, such as ciliary movement and mucus secretion, which are critical for understanding bronchial epithelial injury during transplantation. Conversely, animal models provide a closer mimicry of clinical scenarios but are limited by technical challenges, ethical concerns, high costs, and significant inter-animal variability [15, 41].

The ALI model bridges the gap between these approaches by cultivating primary bronchial epithelial cells in a physiologically relevant setting that allows for differentiation and the development of functional characteristics, including cilia and mucus production. In this study, the ALI model successfully simulated CI/R-induced injury, enabling the evaluation of 4-OI's protective effects on bronchial epithelial morphology and function. By providing a controlled environment to study epithelial-specific responses while retaining some in vivo features, the ALI model offers a powerful tool for exploring lung transplantation-related interventions. Its ability to balance physiological relevance with experimental

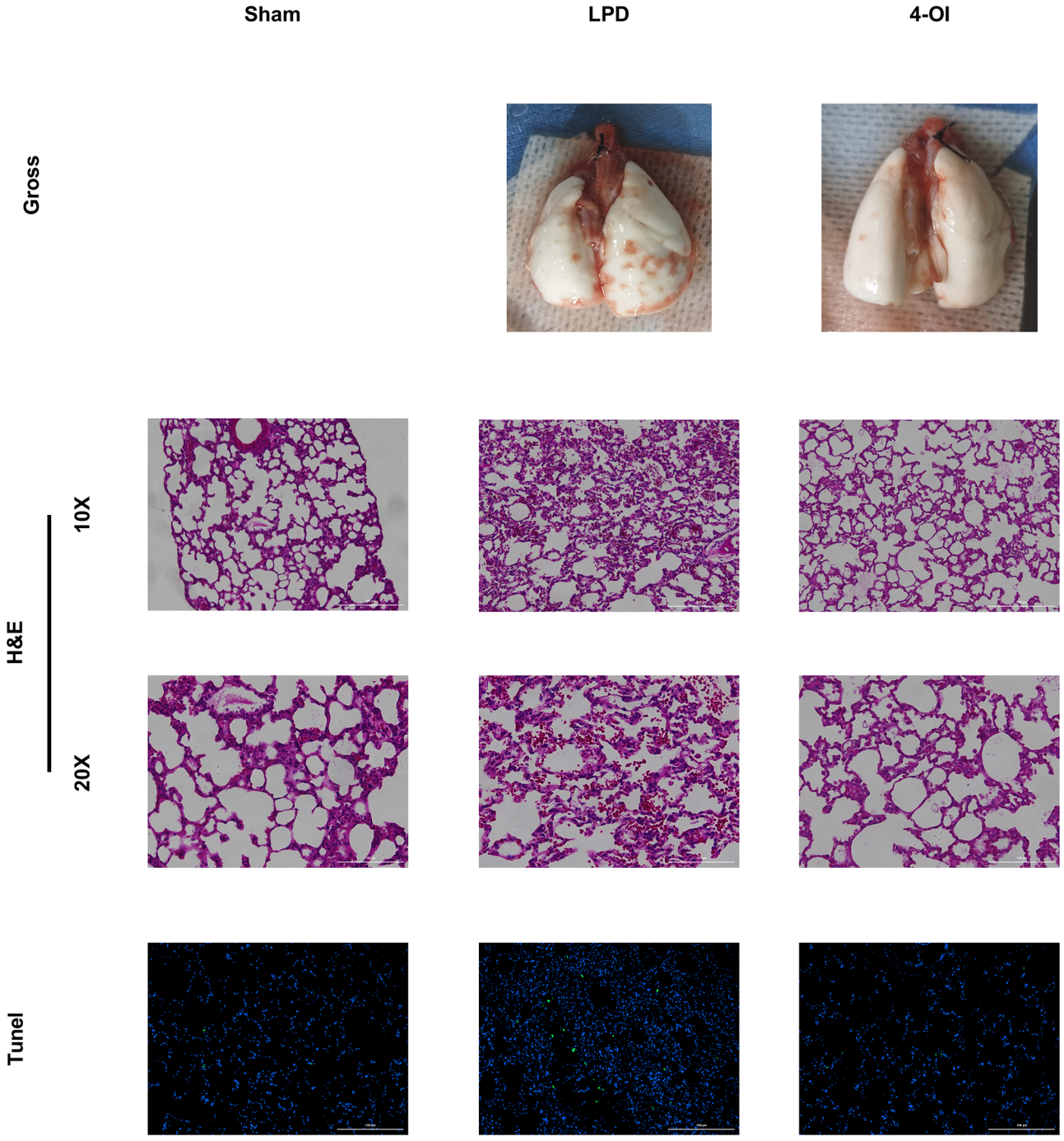

Fig. 7 Protective effect of 4-OI in preservation solution on NHB transplanted lung

feasibility underscores its potential as a complementary approach to existing models in lung transplantation research.

Despite these promising findings, several limitations of this study should be addressed in future research. First, while the protective effects of 4-OI were shown to be largely mediated through Nrf2 activation, its potential non-Nrf2-mediated mechanisms, such as protein alkylation and broader metabolic pathway alterations, remain unexplored. Future studies integrating metabolomics and transcriptomics could provide a more comprehensive understanding of 4-OI's protective mechanisms in lung transplantation. Second, this study primarily focused on the immediate effects of 4-OI during the early reperfusion period. The long-term impact of 4-OI on graft function and survival, including its efficacy in

Table 3 Enhancing rat transplanted lung Protection through Cold Preservation Solution with 4-OI

Injury	Sham	EC LPD	EC 4-OI	NHB LPD	NHB 4-OI	*P* value EC LPD vs. Sham	*P* value EC 4-OI vs. EC LPD	*P* value NHB LPD vs. Sham	*P* value NHB 4-OI vs. NHB LPD
PO_2/FiO_2	388.3 ± 14.2	213.6 ± 30.8	285.7 ± 30.0	185.5 ± 32.5	281.8 ± 27.5	< 0.0001	0.0006	< 0.0001	< 0.0001
W/D ratio	3.7 ± 0.1	5.4 ± 0.7	4.4 ± 0.5	5.7 ± 0.8	4.7 ± 0.5	0.0002	0.0234	< 0.0001	0.0237
Lung injury score	2.2 ± 0.5	7.8 ± 1.0	5.2 ± 1.5	8.9 ± 0.7	5.6 ± 1.2	< 0.0001	0.0007	< 0.0001	< 0.0001
Tunel-positive cells/field	1.2 ± 1.2	14.2 ± 5.3	5.8 ± 3.1	17.0 ± 4.0	5.3 ± 2.5	< 0.0001	0.0014	< 0.0001	< 0.0001
Serum IL-1β (pg/ml)	62.0 ± 7.9	183.0 ± 52.5	82.7 ± 25.5	338.8 ± 90.1	121.1 ± 43.8	0.0018	0.0104	< 0.0001	< 0.0001
Serum IL-6 (pg/ml)	1059.7 ± 192.8	5485.6 ± 1078.1	4336.6 ± 600.8	3436.5 ± 888.3	1844.3 ± 720.7	< 0.0001	0.0569	< 0.0001	0.0049
Serum IL-8 (pg/ml)	52.8 ± 9.5	141.6 ± 57.3	147.2 ± 53.4	200.6 ± 69.4	210.3 ± 60.9	0.0356	0.9996	0.0003	0.9966
Serum TNFα (pg/ml)	159.7 ± 33.0	528.9 ± 110.3	316.7 ± 98.6	499.8 ± 94.7	373.2 ± 55.7	< 0.0001	0.0007	< 0.0001	0.0578

preventing primary graft dysfunction (PGD), requires validation using extended survival models, such as 72-hour or longer post-transplant evaluations. These models would provide critical insights into the sustained benefits and potential risks of 4-OI application in lung transplantation. Finally, this study did not evaluate the potential side effects of 4-OI, particularly its impact on immune responses and infection susceptibility. Considering the pivotal role of immune competence in lung transplant recipients, future studies should investigate the immunomodulatory and potential immunosuppressive effects of 4-OI. These studies could help determine its safety profile and identify strategies to mitigate any adverse effects while preserving its protective benefits.

Conclusions

Adding 4-OI to preservation solutions has shown promising effects in activating Nrf2 pathway to mitigate and mitigating oxidative stress, inflammation, and apoptosis associated with IRI. This intervention helps preserve bronchial epithelial integrity and enhances the function of transplanted lungs. Our study provides a basis for further investigation into the anti-IRI potential of 4-OI in lung transplantation, offering valuable insights for its potential clinical application in this context.

Abbreviations

4-OI	4-octyl itaconate
ALI-airway	Air-liquid interface cultured airway
ARE	Antioxidant response element
ATP	Adenosine triphosphate
CBF	Ciliary beat frequency
CI/R	Cold ischemia/reperfusion injury
DEGs	Differentially expressed genes
EC	Extended cold preservation
ELISA	Enzyme linked immunosorbent assay
GO	Gene ontology
H&E	Hematoxylin and eosin staining
HMOX1	Heme oxygenase 1
IRG1	Immune-responsive gene 1
IRI	Ischemia reperfusion injury
Keap1	Kelch like ECH associated protein 1
LPD	Low potassium dextran solution
LPS	Lipopolysaccharide
NHB	Non-heart beating
NQO1	NAD(P)H quinone oxidoreductase 1
Nrf2	Nuclear factor E2-related factor 2
P/F	PO2/FiO2
PEEP	Positive end-expiratory pressure
PGD	Primary graft dysfunction
ROS	Reactive oxygen species
RT-PCR	Reverse transcription polymerase chain reaction
SLC7A11	Solute Carrier Family 7 Member 11
TEER	Trans-epithelial electric resistance
TUNEL	TdT-mediated dUTP nick end labeling
W/D	Wet/dry ration
WB	Western blotting

Supplementary Information

The online version contains supplementary material available at https://doi.org/10.1186/s12931-025-03151-7.

Supplementary Material 1

Supplementary Material 2

Supplementary Material 3

Supplementary Material 4

Supplementary Material 5

Acknowledgements

The authors are very grateful to the patients for participating in this study and donating their biological samples.

Author contributions

Xinliang Gao and Wei Liu participated in research design. Xinliang Gao and Mingbo Tang participated in the writing of the paper. Xinliang Gao, Jialin Li and Jianzun Ma participated in the performance of the research. Zhengrui Liu contributed new reagents or analytic tools. Xinliang Gao and Mingbo Tang participated in data analysis.

Funding

This study was supported by the Scientific Research Project of Jilin Provincial Department of Education (No. JJKH20231215KJ).

Data availability
Sequence data that support the findings of this study have been deposited in the GSA for human in National Genomics Data Center with the accession code HRA008064. (https://ngdc.cncb.ac.cn/gsa-human/s/tK584YnN).

Declarations

Ethics approval and consent to participate
The research involving human tissue in this study was approved by the Institutional Ethics Committees of The First Hospital of Jilin University for tissue usage (approval number: 2024 – 479). All animal procedures were approved and performed according to the protocols established by the Institutional Animal Care and Use Committee of The First Hospital of Jilin University (approval number: 2023[0636]).

Consent for publication
Not applicable.

Competing interests
The authors declare no competing interests.

Received: 23 July 2024 / Accepted: 11 February 2025
Published online: 27 February 2025

References

1. Bos S, Vos R, Van Raemdonck DE, Verleden GM. Survival in adult lung transplantation: where are we in 2020? Curr Opin Organ Transpl. 2020;25:268–73.
2. Diamond JM, Arcasoy S, Kennedy CC, Eberlein M, Singer JP, Patterson GM, Edelman JD, Dhillon G, Pena T, Kawut SM, et al. Report of the International Society for Heart and Lung Transplantation Working Group on Primary Lung Graft Dysfunction, part II: epidemiology, risk factors, and outcomes-A 2016 Consensus Group statement of the International Society for Heart and Lung Transplantation. J Heart Lung Transpl. 2017;36:1104–13.
3. Diamond JM, Lee JC, Kawut SM, Shah RJ, Localio AR, Bellamy SL, Lederer DJ, Cantu E, Kohl BA, Lama VN, et al. Clinical risk factors for primary graft dysfunction after lung transplantation. Am J Respir Crit Care Med. 2013;187:527–34.
4. Ali A, Wang A, Ribeiro RVP, Beroncal EL, Baciu C, Galasso M, Gomes B, Mariscal A, Hough O, Brambate E, et al. Static lung storage at 10°C maintains mitochondrial health and preserves donor organ function. Sci Transl Med. 2021;13:eabf7601.
5. Chambers DC, Yusen RD, Cherikh WS, Goldfarb SB, Kucheryavaya AY, Khusch K, Levvey BJ, Lund LH, Meiser B, Rossano JW, Stehlik J. The Registry of the International Society for Heart and Lung Transplantation: thirty-fourth adult lung and heart-lung transplantation Report-2017; focus theme: allograft ischemic time. J Heart Lung Transpl. 2017;36:1047–59.
6. Keshavjee SH, Yamazaki F, Cardoso PF, McRitchie DI, Patterson GA, Cooper JD. A method for safe twelve-hour pulmonary preservation. J Thorac Cardiovasc Surg. 1989;98:529–34.
7. Liu WC, Chen SB, Liu S, Ling X, Xu QR, Yu BT, Tang J. Inhibition of mitochondrial autophagy protects donor lungs for lung transplantation against ischaemia-reperfusion injury in rats via the mTOR pathway. J Cell Mol Med. 2019;23:3190–201.
8. Chouchani ET, Pell VR, Gaude E, Aksentijević D, Sundier SY, Robb EL, Logan A, Nadtochiy SM, Ord ENJ, Smith AC, et al. Ischaemic accumulation of succinate controls reperfusion injury through mitochondrial ROS. Nature. 2014;515:431–5.
9. Shi X, Zhou H, Wei J, Mo W, Li Q, Lv X. The signaling pathways and therapeutic potential of itaconate to alleviate inflammation and oxidative stress in inflammatory diseases. Redox Biol. 2022;58:102553.
10. Mills EL, Ryan DG, Prag HA, Dikovskaya D, Menon D, Zaslona Z, Jedrychowski MP, Costa ASH, Higgins M, Hams E, et al. Itaconate is an anti-inflammatory metabolite that activates Nrf2 via alkylation of KEAP1. Nature. 2018;556:113–7.
11. Su C, Cheng T, Huang J, Zhang T, Yin H. 4-Octyl itaconate restricts STING activation by blocking its palmitoylation. Cell Rep. 2023;42:113040.
12. Lei I, Huang W, Noly PE, Naik S, Ghali M, Liu L, Pagani FD, Abou El Ela A, Pober JS, Pitt B, et al. Metabolic reprogramming by immune-responsive gene 1 up-regulation improves donor heart preservation and function. Sci Transl Med. 2023;15:eade3782.
13. Jing L, Konoeda H, Keshavjee S, Liu M. Using nutrient-rich solutions and adding multiple cytoprotective agents as new strategies to develop lung preservation solutions. Am J Physiol Lung Cell Mol Physiol. 2021;320:L979–89.
14. Ninaber DK, van der Does AM, Hiemstra PS. Isolating bronchial epithelial cells from resected lung tissue for biobanking and establishing well-differentiated air-liquid interface cultures. J Vis Exp. 2023;26:(195).
15. Tian D, Shiiya H, Sato M, Nakajima J. Rat lung transplantation model: modifications of the cuff technique. Ann Transl Med. 2020;8:407.
16. Lee YG, Kim JL, Palmer AF, Reader BF, Ma J, Black SM, Whitson BA. A rat lung transplantation model of warm ischemia/reperfusion injury: optimizations to improve outcomes. J Vis Exp. 2021;28:(176).
17. Kanou T, Ohsumi A, Kim H, Chen M, Bai X, Guan Z, Hwang D, Cypel M, Keshavjee S, Liu M. Inhibition of regulated necrosis attenuates receptor-interacting protein kinase 1-mediated ischemia-reperfusion injury after lung transplantation. J Heart Lung Transpl. 2018;37:1261–70.
18. Cypel M, Rubacha M, Yeung J, Hirayama S, Torbicki K, Madonik M, Fischer S, Hwang D, Pierre A, Waddell TK, et al. Normothermic ex vivo perfusion prevents lung injury compared to extended cold preservation for transplantation. Am J Transpl. 2009;9:2262–9.
19. Duan X, Liu X, Liu N, Huang Y, Jin Z, Zhang S, Ming Z, Chen H. Inhibition of keratinocyte necroptosis mediated by RIPK1/RIPK3/MLKL provides a protective effect against psoriatic inflammation. Cell Death Dis. 2020;11:134.
20. Zhao X, Feng R, Chen J, Jiang Q, Hua X, Liang C. 4-Octyl itaconate alleviates experimental autoimmune prostatitis by inhibiting the NLRP3 inflammasome-induced pyroptosis through activating Nrf2/HO-1 pathway. Prostate. 2024;84:329–41.
21. Cui BC, Aksenova M, Sikirzhytskaya A, Odhiambo D, Korunova E, Sikirzhytski V, Ji H, Altomare D, Broude E, Frizzell N et al. Suppression of HIV and cocaine-induced neurotoxicity and inflammation by cell penetrable itaconate esters. bioRxiv 2023.
22. Yang W, Wang Y, Wang T, Li C, Shi L, Zhang P, Yin Y, Tao K, Li R. Protective effects of IRG1/itaconate on acute colitis through the inhibition of gasdermins-mediated pyroptosis and inflammation response. Genes Dis. 2023;10:1552–63.
23. Zhang Q, Bai X, Wang R, Zhao H, Wang L, Liu J, Li M, Chen Z, Wang Z, Li L, Wang D. 4-octyl Itaconate inhibits lipopolysaccharide (LPS)-induced osteoarthritis via activating Nrf2 signalling pathway. J Cell Mol Med. 2022;26:1515–29.
24. Xin L, Zhou F, Zhang C, Zhong W, Xu S, Jing X, Wang D, Wang S, Chen T, Song J. Four-octyl itaconate ameliorates periodontal destruction via Nrf2-dependent antioxidant system. Int J Oral Sci. 2022;14:27.
25. Kim HW, Yu AR, Lee JW, Yoon HS, Lee BS, Park HW, Lee SK, Lee YI, Whang J, Kim JS. Aconitate decarboxylase 1 deficiency exacerbates mouse colitis induced by dextran sodium sulfate. Int J Mol Sci. 2022;23(8):4392.
26. Pan X, Shan H, Bai J, Gao T, Chen B, Shen Z, Zhou H, Lu H, Sheng L, Zhou X. Four-octyl itaconate improves osteoarthritis by enhancing autophagy in chondrocytes via PI3K/AKT/mTOR signalling pathway inhibition. Commun Biol. 2022;5:641.
27. Wang Q, Ye X, Tan S, Jiang Q, Su G, Pan S, Li H, Cao Q, Yang P. 4-Octyl Itaconate Inhibits Pro-inflammatory Cytokine Production in Behcet's Uveitis and Experimental Autoimmune Uveitis. Inflammation 2024.
28. He S, Zhao Y, Wang G, Ke Q, Wu N, Lu L, Wu J, Sun S, Jin W, Zhang W, Zhou J. 4-Octyl itaconate attenuates glycemic deterioration by regulating macrophage polarization in mouse models of type 1 diabetes. Mol Med. 2023;29:31.
29. Wang X, Kong W, Yang R, Yang C. 4-octyl itaconate ameliorates ventilator-induced lung injury. Arch Biochem Biophys. 2024;752:109853.
30. Xie Y, Chen Z, Wu Z. Four-Octyl Itaconate Attenuates UVB-Induced Melanocytes and Keratinocytes Apoptosis by Nrf2 Activation-Dependent ROS Inhibition. Oxid Med Cell Longev 2022, 2022:9897442.
31. Wang L, Chen Z, Feng Y, Wang R, Bai X, Liu W, Wang D. RNA-seq transcriptomic analysis of 4-octyl itaconate repressing myogenic differentiation. Arch Biochem Biophys. 2022;731:109420.
32. Hu Z, Xu D, Meng H, Liu W, Zheng Q, Wang J. 4-octyl itaconate protects against oxidative stress-induced liver injury by activating the Nrf2/Sirt3 pathway through AKT and ERK1/2 phosphorylation. Biochem Pharmacol. 2024;220:115992.
33. Chen G, Li J, Liu H, Zhou H, Liu M, Liang D, Meng Z, Gan H, Wu Z, Zhu X, et al. Cepharanthine ameliorates pulmonary fibrosis by inhibiting the NF-κB/NLRP3 pathway, fibroblast-to-myofibroblast transition and inflammation. Molecules. 2023;28(2):753.

34. Xu L, Cai J, Li C, Yang M, Duan T, Zhao Q, Xi Y, Sun L, He L, Tang C, Sun L. 4-Octyl itaconate attenuates LPS-induced acute kidney injury by activating Nrf2 and inhibiting STAT3 signaling. Mol Med. 2023;29:58.
35. Zhang P, Wang X, Peng Q, Jin Y, Shi G, Fan Z, Zhou Z. Four-Octyl Itaconate protects chondrocytes against H(2)O(2)-Induced oxidative Injury and attenuates osteoarthritis progression by activating Nrf2 signaling. Oxid Med Cell Longev. 2022;2022:2206167.
36. Chiabrando D, Vinchi F, Fiorito V, Mercurio S, Tolosano E. Heme in pathophysiology: a matter of scavenging, metabolism and trafficking across cell membranes. Front Pharmacol. 2014;5:61.
37. Jeney V, Balla J, Yachie A, Varga Z, Vercellotti GM, Eaton JW, Balla G. Pro-oxidant and cytotoxic effects of circulating heme. Blood. 2002;100:879–87.
38. Eizirik DL, Flodström M, Karlsen AE, Welsh N. The harmony of the spheres: inducible nitric oxide synthase and related genes in pancreatic beta cells. Diabetologia. 1996;39:875–90.
39. Dong H, Xia Y, Jin S, Xue C, Wang Y, Hu R, Jiang H. Nrf2 attenuates ferroptosis-mediated IIR-ALI by modulating TERT and SLC7A11. Cell Death Dis. 2021;12:1027.
40. Feng L, Zhao K, Sun L, Yin X, Zhang J, Liu C, Li B. SLC7A11 regulated by NRF2 modulates esophageal squamous cell carcinoma radiosensitivity by inhibiting ferroptosis. J Transl Med. 2021;19:367.
41. Mariscal A, Caldarone L, Tikkanen J, Nakajima D, Chen M, Yeung J, Cypel M, Liu M, Keshavjee S. Pig lung transplant survival model. Nat Protoc. 2018;13:1814–28.

Publisher's note

Springer Nature remains neutral with regard to jurisdictional claims in published maps and institutional affiliations.